Journal of Theoretical and Applied Mechanics, Sofia, Vol.52 (2022) pp. 64-74
SOLID MECHANICS

MODELLING OF ULTRASONIC TEMPORARY AND RESIDUAL EFFECTS

ALI H. ALHILFI[1], ANDREW RUSINKO[2*],
[1]*Misan University, Iraq*
[2]*Obuda University, Nepszinhaz St. 8, Budapest, H-1081 Hungary*

[Received: 28 October 2020. Accepted: 20 September 2021]
doi: https://doi.org/10.55787/jtams.22.52.1.064

ABSTRACT: This study discusses the phenomena of ultrasonic temporary softening and ultrasonic residual hardening registered in the experiments for plastic deformation of metals in ultrasonic field. This paper is aimed to model these phenomena in terms of the synthetic theory of irrecoverable deformation. We extend the flow rule relationships by two terms constructed on the base of microstructural processes occurring in ultrasound assisted deformation. The model results show good agreement with experimental data.

KEY WORDS: ultrasound, plastic deformation, residual hardening, residual softening.

1 INTRODUCTION

As a result of the high efficiency and simple implementation of ultrasound, it has been widely accepted in the fields of biomedicine, chemistry, metal forming and metallurgy. The principle underlying the effect of ultrasound is that, when a sound wave propagates through a substance, the acoustic energy is being scattered and absorbed by the material, the sound waves interfere with its defects.

A number of studies relating the effect of ultrasound upon the deformation properties of metals can be resumed by Zhou et al. results shown in Figs. 1 and 2 [1].

Two portions can be identified:

(i) Ultrasound assisted deformation (acoustoplasticity).

The plastic flow of both aluminum and titanium takes place at stresses less compared to the ordinary loading (Figs. 1 and 2, US-on). This phenomenon is referred to as ultrasonic temporary softening.

Numerous positive effects from using ultrasound are reported by the researchers. Hung [2] have studied the assistance of ultrasound vibrations in hot upsetting of aluminum alloys. It is found that the required compressive forces are declined by the

*Corresponding author e-mail: ruszinko.endre@bgk.uni-obuda.hu

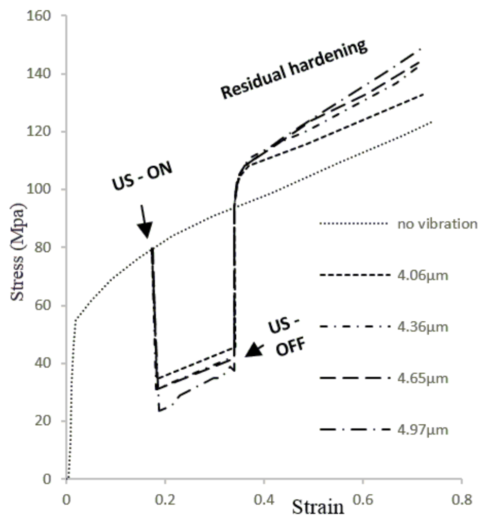

Fig. 1: Stress vs strain diagrams of aluminum in the ultrasonic field of various oscillation amplitudes [1].

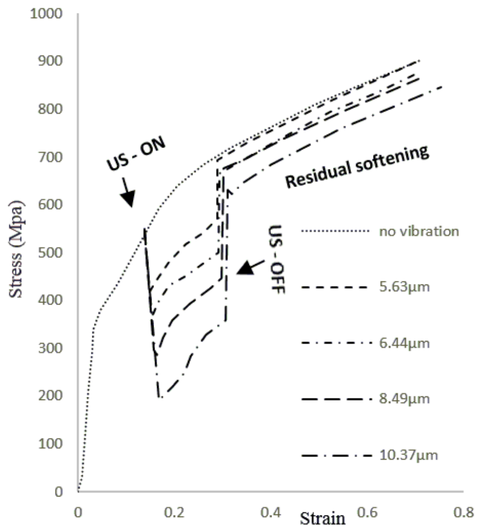

Fig. 2: Stress vs strain diagrams of titanium in the ultrasonic field of various oscillation amplitudes [1].

effect of ultrasonic vibration during hot upsetting. Crinkling and cracking could be avoided by using ultrasonic energy supplied to the die of press forming, according to Ashida and Aoyama [3]. Jimma et al. [4] studied the effect of ultrasonic assisted deep drawing processes and found that ultrasonic energy increases the ratio of limiting drawing and reduce the drawing force. Improving the lubrication condition between the wire and die and the drawing force reduction is reported by Lianshi [5] due to ultrasonic energy. Simulations were performed by Lucas and Daud [6] for ultrasonic assisted extrusion of aluminum.

(ii) Deformation in post-sonicated period (Figs. 1 and 2, US-off).

According to numerous investigations conducted for Zn [7], Cu [8], Mg [9], Au [10], cold rolled steels [11], it can be argued that high frequency vibration can permanently change the mechanical properties of metals, which results in so called ultrasonic residual effects.

Yao et al. [12] developed a crystal plasticity-based model for modelling the ultrasonic assisted compression test of aluminum. They interpreted the residual hardening effect by the ultrasound assisted multiplication of the defects of crystalline lattice. Similarly to Yao, Zhou et al. [1], via EBSD tests, found that for aluminum the ultrasonic vibration reduced the grain size and changed the orientation of the grains. As a result, it may be concluded that excess of defects nucleated in ultrasonic field impede the development of plastic deformation after the ultrasound is off.

The ultrasonic residual softening effect is mentioned as the possible result of softening mechanisms dominating during the simultaneous action of vibrating and unidirectional loading. Lum et al. [10], conducting experiments for ultrasonic wire bonding of gold, explained that the ultrasonic vibration could induce sufficient heat input to the sample to make it recrystallize and reduce the dislocation density; hence there was a residual softening effect. Huang et al. reported similar results for cooper, when studied the residual softening effect during the ultrasonic wire bonding [13].

The softening mechanism for titanium [1] was derived from the study of the fraction of twinning boundaries, which are abundant in many metals with low stacking fault energy (SFE) such as titanium, copper, gold etc. It was reported that the ultrasonic vibration promotes the saturation of twinning and reduce the fraction of twinning boundaries. Since the twinning boundary works as a hardening factor to titanium, the titanium sample exhibits a residual softening effect with less twinning boundaries.

From the short review of experimental results above, the conclusion cannot be escaped that, at least in terms of experiments considered, the metals with high SFE, such as, e.g., aluminum, are inclined to ultrasonic residual hardening. In contrast, metals with low SFE (titanium, copper, gold) manifest the phenomenon of ultrasonic residual softening.

This work is step forward in our research of modeling the effect of ultrasound on the plastic deformation of metals which is started with Rusinko [14] in terms of the synthetic theory of irrecoverable deformation [15]. In contrast to [14], where the ultrasonic temporary softening alone is modelled, here we discuss a more complicated case obtained by Zhou et al. [1] which, in addition to acoustic temporary softening, involves the residual softening for titanium and the residual hardening for aluminum.

2 Synthetic Theory

In terms of this theory [15], plastic deformation at a point of body is determined via deformations at the microlevel of material, i.e. as a sum of plastic shifts in active slips systems where the resolved shear stress exceeds the material yield strength (the Schmidt law)

$$\vec{e} = \iiint\limits_V \varphi_N \vec{N} dV \,, \tag{1}$$

where φ_N – plastic strain intensity – is an average measure of plastic deformation within one slip system.

The main feature of the synthetic theory is the formulation of yield criterion and strain hardening rule in terms of three-dimensional stress deviator space (S^3). To be specific, we do not deal with a yield surface itself – for initial state we take the von-Mises criterion – but with its tangent planes, i.e. the yield surface is considered as an inner envelope of the tangent planes. The location of planes is defined by their distances (H_N) and unit normal vectors ($\vec{N}$). Loading is exhibited by a stress vector ($\vec{S}$). During loading, the stress vector shifts at its endpoint a set of planes from their initial position. The movements of the planes lying at the endpoint of vector $\vec{S}$ are translational. Planes which are not located at the endpoint of vector $\vec{S}$ remain stationary. The displacement of plane at the endpoint of stress vector represents a plastic flow within corresponding slip system.

The plastic flow rule on the micro level of material is [15]

$$
\begin{aligned}
r\varphi_N &= H_N^2 - S_S^2 \\
&= \begin{cases} (\vec{S}\cdot\vec{N})^2 - S_S^2 & \text{for planes reached by } \vec{S}: H_N = \vec{S}\cdot\vec{N} \\ 0 & \text{for planes not reached by } \vec{S}: H_N > \vec{S}\cdot\vec{N} \end{cases}.
\end{aligned} \tag{2}
$$

The scalar product $\vec{S}\cdot\vec{N}$ defines the resolved shear stress acting in one slip system. The plane distance H_N represents the hardening of material, because the greater H_N is, the grater $\vec{S}$ is needed to reach the plane. In Eq. (2), $S_S = \sqrt{2/3}\sigma_S$, where σ_S is the yield strength of material; r is the model constant determining the slope of stress$\sim$strain curves; $[r] = \mathrm{MPa}^2$.

The results obtained for uniaxial tension [14] can be also utilized for compression, by using the advantage that the isotropy postulate holds in terms of the synthetic theory. So, the loading is indicated by stress vector $\vec{S}\left(\sqrt{2/3}\sigma, 0, 0\right)$ which extend along the S_1 axis, and $H_N = S_1 N_1 = \sqrt{2/3}\sigma\sin\beta\cos\lambda$. Eqs. (1) and (2) take the following form [15]:

$$\varphi_N = \frac{2}{3r}\left[(\sigma\sin\beta\cos\lambda)^2 - \sigma_S^2\right], \tag{3}$$

$$e = \frac{4\pi}{3r}\int\limits_{\beta_1}^{\pi/2}\int\limits_{0}^{\lambda_1}\left[(\sigma\sin\beta\cos\lambda)^2 - \sigma_S^2\right]\sin\beta\cos\lambda\cos\beta d\lambda d\beta = a_0\Phi\left(b\right), \tag{4}$$

where

$$a_0 = \frac{\pi\sigma_S^2}{9r_0}, \quad \Phi(b) = \frac{1}{b^2}\left[2\sqrt{1-b^2} - 5b^2\sqrt{1-b^2} + 3b^4\ln\frac{1+\sqrt{1-b^2}}{b}\right]. \tag{5}$$

The integration boundaries in (4) are obtained from (3) by letting $\varphi_N = 0$ and $\lambda = 0$

$$\sin\beta_1 = \frac{\sigma_S}{\sigma} \equiv b, \qquad \cos\lambda_1 = \frac{\sigma_S}{\sigma \sin\beta}\,. \tag{6}$$

If to add σ/E to e from (4), we obtain the total deformation at the stress σ.

3 Synthetic Theory for the Case of Plastic Straining with Ultrasound

For the purpose of modeling the effects of ultrasound on the plastic strain of metals, we extend Eq. (2) by two terms, U_t and U_r

$$r\varphi_{NU} = H_N^2 + U_t^2 + f(\gamma)U_r^2 - S_S^2\,. \tag{7}$$

U_t represents the temporary softening action of ultrasound, and its presence in the formula above makes it possible to maintain a given value of strain intensity at less value of unidirectional stress. We define U_t as

$$U_t = A_1\sigma_m^{A_2}\left(2 - e^{-pt}\right)\left(\vec{u}\cdot\vec{N}\right), \quad t \in [0, \tau], \tag{8}$$

where σ_m is the vibrating stress amplitude [MPa], $\vec{u}$ is the unit vector indicating the vibration mode (longitudinal, torsional, etc.). For longitudinal sonication, the $\vec{u}$ vector has $(1, 0, 0)$ coordinates in S^3. Further, τ is the sonication duration, and p and A_k $(k = 1, 2)$ are model constants. If to denote through $\vec{U}$ the vector $A_1\sigma_m^{A_2}\left(2 - e^{-pt}\right)\vec{u}$, Eq. (8) becomes $U_t = \vec{U}\cdot\vec{N}$, i.e. the action of ultrasound is presented by a vector, whose component depends on vibration amplitude and time.

Equation (8) correlates with numerous investigations – [1, 10, 13, 16] – reporting that the magnitude of ultrasonic temporary softening is governed by the amplitude of oscillating stress. It is the power function $2A_1\sigma_m^{A_2}$ that links the stress amplitude to the temporary softening effect.

Temporary development of softening effect is expressed in U_t via exponential function. As a result, the term $A_1\sigma_m^{A_2}e^{-pt}$ correlates with the temporary multiplication of ultrasound induced defects (ψ_{NU}) proposed by Rusinko [14]. The decreasing fashion of e^{-pt} function expresses experimental facts that the number of defects increases with time till they reach a plateau [9, 16].

Therefore, Eq. (8) is of dual nature. On the one hand, the ultrasound defects harden the material, but, on the other hand, they become centers of softening processes. As evident from (8), since the term $\left(2-e^{-pt}\right)$ is always positive, the net effect is a prevalence of softening mechanisms during simultaneous action of unidirectional and oscillating load.

The term $f(\gamma)\,U_r^2$ in Eq. (7) models the deformation properties of metals after the ultrasound is off, i.e. residual effects. Its effect depends on the sign of $f(\gamma)$ function, where γ is stacking fault energy. If to define $f(\gamma)$ as a decreasing function of γ, it takes a negative value for high stacking fault energies. In this case we obtain the situation of residual ultrasonic hardening, because the negative term $f(\gamma)\,U_r^2$ in Eq. (7) suppresses the development of plastic slips φ_{NU}. Or vice versa, for positive values of $f(\gamma)$, which is typical for materials with small γ, we arrive at the case of residual softening. We define U_r as a stress and time dependent function

$$U_r = h(\varepsilon - \sigma_m) \times A_3 \int_0^{\tau} \sigma_m^{A_4} dt, \tag{9}$$

where h is the Heaviside step function, ε is any positive infinitesimally small number so that ultrasound of any intensity results in negative value of $\varepsilon - \sigma_m$ difference. The presence of $h(\varepsilon - \sigma_m)$ function means that the U_r term takes effect only after the ultrasound is off. Again, we propose a power function to express the dependence of ultrasonic residual hardening upon the ultrasound intensity with model constants A_3 and A_4. At the same time, the intensity of sonication is not the only parameter governing the magnitude of hardening effect. Namely, the duration of sonication plays an important role as well, in other words, the time-integral in (9) reflects the time dependent magnitude of ultrasonic energy injected into material.

Summarizing, U_r reflects a post-sonicated-defect-pattern leading to the change in material characteristics/response after the acoustoplasticity.

4 Uniaxial Stress State

4.1 Acoustoplasticity ($\sigma > 0 \bigwedge \sigma_m > 0$)

For vibrating-assisted deformation, $t \in [0, \tau]$, U_t increases in the way prescribed by (8). At the same time, due to $h = 0$ in (9), we have $U_r = 0$ during the action of ultrasound.

So, Eq. (7) takes the following form:

$$\begin{aligned} r\varphi_{NU} &= H_N^2 + U_t^2 - S_S^2 = (\vec{S}\cdot\vec{N})^2 + \left[A_1\sigma_m^{A_2}(2-e^{-pt})(\vec{u}\bullet\vec{N})\right]^2 - S_S^2 \\ &= \frac{2}{3}\left[(\sigma_U \sin\beta\cos\lambda)^2 + \frac{3}{2}\left[A_1\sigma_m^{A_2}(2-e^{-pt})\sin\beta\cos\lambda\right]^2 - \sigma_S^2\right]. \end{aligned} \tag{10}$$

Plastic deformation in acoustoplasticity (e_U) is calculated by Eq. (1) with the integrand from (10). As a result,

$$e_U = a_0 \Phi\left(b_U\right), \qquad (11)$$
$$b_U = \frac{\sigma_S}{\sqrt{\sigma_U^2 + \frac{3}{2}\left(A_1 \sigma_m^{A_2}\left(2 - e^{-pt}\right)\right)^2}}.$$

Comparing Eq. (11) with (5) and (6), we conclude that the deforming of material in ultrasonic field develops at less unidirectional stress σ_U compared to that under ordinary loading. Consequently, Eqs. (10) and (11) describe analytically the phenomenon of temporary ultrasonic softening.

4.2 Post-sonicated deformation ($\sigma > 0 \bigwedge \sigma_m = 0$)

While, due to $\sigma_m = 0$ for $t > \tau$, $U_t = 0$, the integral from (9) gives nonzero value ($h(\varepsilon)= 1 \Rightarrow U_r > 0$).

Comparing to (10), the plastic strain intensity loses the term U_t, which facilitated the strain intensity, but includes U_r:

$$r\varphi_{Nr} = H_N^2 + f(\gamma) U_r^2 - S_S^2. \qquad (12)$$

Since, so far, there is no enough experimental data on the effect of SFE upon the post-sonicated deformation for a wide range of metals, we propose a linear relationship for $f(\gamma)$ related to the value of SFE for aluminum:

$$f(\gamma) = k(\gamma_{\text{Al}} - \gamma) - 1\,, \qquad (13)$$

where $k \geq 1$ is a model constant. Taking into account the range of SFE of metals considered, we obtain that $f(\gamma_{\text{Al}}) = -1$, and $f(\gamma_{\text{Ti}})$ takes a positive value because $\gamma_{\text{Al}} > \gamma_{\text{Ti}}$.

Now, Eq. (12) takes the following shapes for aluminum and titanium, respectively:

$$r\varphi_{Nr} = \frac{2}{3}\left[\left(\sigma \sin\beta \cos\lambda\right)^2 - \frac{3}{2}\left[A_3 \sigma_m^{A_4} \tau\right]^2 - \sigma_S^2\right], \qquad (14)$$

$$r\varphi_{Nr} = \frac{2}{3}\left[\left(\sigma \sin\beta \cos\lambda\right)^2 + \frac{3}{2} f\left(\gamma_{\text{Ti}}\right)\left[A_3 \sigma_m^{A_4} \tau\right]^2 - \sigma_S^2\right]. \qquad (15)$$

The deformation of both aluminum and titanium specimens is calculated via formula (1), with the difference being that the strain intensity φ_N is governed by Eq. (14) and Eq. (15), respectively.

Comparing formula (14) to (3), it is obvious that $\varphi_{Nr} < \varphi_N$, i.e. the stress∼strain curve runs above that corresponding to ordinary loading. Therefore, formula (14) models the phenomenon of ultrasonic residual hardening, which is observed for aluminum.

With titanium, it is clear from (15) and (3) that $\varphi_{Nr} > \varphi_N$, i.e. the stress∼strain curve locates beneath that where unidirectional load acts alone. Here, we obtain the case of ultrasonic residual softening.

5 Results

In this section we plot stress∼strain curves obtained in terms of the synthetic theory via formulae developed in previous points. The purpose of this is to compare the analytic results with those obtained by Zhou et al. [1] in ultrasound assisted compression for aluminum and titanium (Figs. 3 and 4).

Aluminum. The first step is to select the appropriate value of r to match the ordinary $\sigma \sim \varepsilon$ diagram (no vibration) to the experimental one. The theoretical $\sigma \sim \varepsilon$ curve from Fig. 3, which is plotted using Eqs. (4)–(6) at $r = 6700$ MPa^2, $E = 70$ Gpa, and $\sigma_S = 45$ MPa, exhibits good agreement with experimental data.

The moment the stress is 79.2 MPa [1], ultrasound of different amplitude (A) is on for 24 seconds ($\tau = 24$ s). The values of A used in the experiment are: 4.06, 4.36, 4.65, 4.97 μm [1]. To calculate the amplitudes of oscillating stress corresponding to

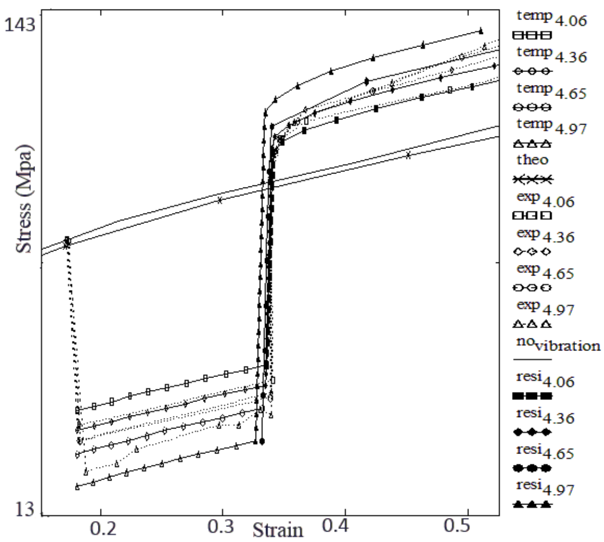

Fig. 3: Stress∼strain compression diagrams of aluminum in the ultrasonic field (“exp“ – experimental data; “temp“ and “resi” – model curves).

A, utilize the following relationship:

(16) $$\sigma_m = E\frac{2\pi f}{c}A\,,$$

where c is the speed of sound ($c = 6,420$ m/s for aluminum), and f is the frequency ($f = 30$ kHz [1]). As a result, $\sigma_{m1} = 8.3$ MPa, $\sigma_{m2} = 8.9$ MPa, $\sigma_{m3} = 9.6$ MPa, $\sigma_{m4} = 10.2$ MPa.

Now, via formula (11), we plot $\sigma \sim \varepsilon$ diagrams under the action of ultrasound. As seen from Fig. 3, constants $A_1 = 1.9515 \times 10^{-2}$ MPa$^{1-A_2}$, $A_2 = 0.5$, $p = 5.5 \times 10^{-3}$ s^{-1}, and $t \in [0, 24]$ in Eq. (11) lead to correct results.

The final step is the deformation of post-sonicated material, which is calculated via Eqs. (14) and (1). These relationships at $A_3 = 2.1 \times 10^{-7}$ MPa$^{1-A_4}$ and $A_4 = 4$ show good agreement with experimental data.

Titanium. The specimens were sonicated with the following amplitudes (A): 5.63, 6.44, 8.49, 10.37 μm [1]. Eq. (16) at $c = 3,300$ m/s gives the following values of stress amplitude: $\sigma_{m1} = 3.2$ MPa, $\sigma_{m2} = 3.68$ MPa, $\sigma_{m3} = 4.85$ MPa, $\sigma_{m4} = 5.9$ MPa.

Similarly to the previous case, first, we choose an appropriate value of r to match the fundamental stress˜strain diagram to the experimental one. Calculations in Eqs. (4)–

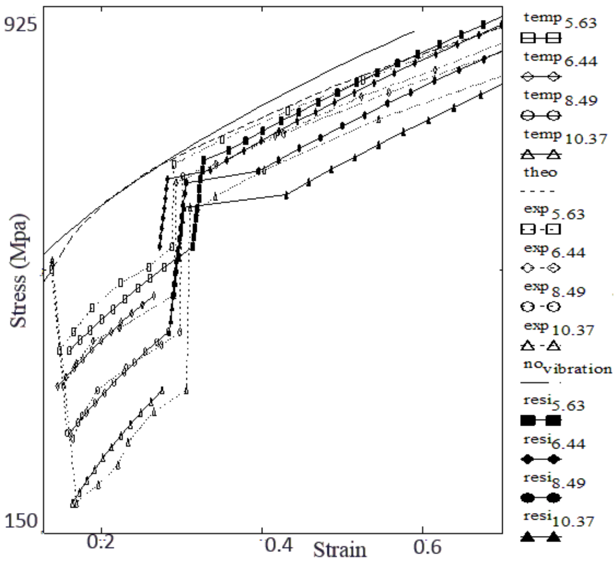

Fig. 4: Stress∼strain compression diagrams of titanium in the ultrasonic field (“exp” – experimental data; “temp” and “resi” – model curves).

(6) at $r = 5.3 \times 10^5$ MPa^2, $E = 10$ Gpa and $\sigma_S = 370$ MPa exhibit good agreement with experimental data (Fig. 2, no vibration). Ultrasound starts when the stress is of 538 MPa [1] and temporary ultrasonic softening is observed ($\tau = 24$ s. Now, Eq. (11) comes into play, which with constants $A_1 = 205$ MPa$^{1-A_2}$, $A_2 = 0.5$, and $p = 1.0 \times 10^{-3}$ s^{-1} leads to correct results.

Finally, we plot $\sigma \sim \varepsilon$ diagrams for the post-sonicated period. If to utilize Eqs. (15) and (1) at $\gamma_{\text{Al}} = 166$ mJ/m^2, $\gamma_{\text{Ti}} = 15$ mJ/m^2, $A_3 = 2.5 \times 10^{-5}$ MPa$^{1-A_4}$, $A_4 = 2$, and $k = 1.0$ m^2/mJ, we achieve the conformity of the analytical and experimental result (see Fig. 4).

6 Conclusion

In this study two phenomena observed during plastic deformation in ultrasonic field are modelled – ultrasonic temporary softening and ultrasonic residual hardening. Synthetic theory of irrecoverable deformation was used to develop a model to predict the stress˜strain curves in ultrasound assisted compression for aluminum and titanium. For this purpose, we extended the flow rule by two terms which govern the plastic deformation of material in ultrasonic field and after the ultrasound is off, respectively. The first term symbolizes the fact that ultrasound facilitates the development of plastic deformation by activation of blocked dislocations, localized heating and dynamic softening. The second one reflects the effect of the defect structure formed during the sonication on the plastic properties of metals for post-sonicated period. Analytical results obtained in terms of the synthetic theory show good agreement with experimental data.

References

[1] H. Zhou, H. Cui, Q.H. Qin (2018) Influence of ultrasonic vibration on the plasticity of metals during compression process. *Journal of Materials Processing Technology* **251** 146-159.

[2] J.C. Hung, C. Hung (2005) The influence of ultrasonic-vibration on hot upsetting of aluminum alloy. *Ultrasonics* **43** 692-698.

[3] Y. Ashida, H. Aoyama (2007) Press forming using ultrasonic vibration. *Journal of Materials Processing Technology* **187** 118-122.

[4] T. Jimma, Y. Kasuga, N. Iwaki, O. Miyazawa, E. Mori, K. Ito, H. Hatano (1998) An application of ultrasonic vibration to the deep drawing process. *Journal of Materials Processing Technology* **80** 406-412.

[5] L. Lianshi, L. Xioping (1994) Wire drawing with ultrasonic vibration. *Wire Industry* **61** 31-33.

[6] M. Lucas, Y. Daud (2009) A finite element model of ultrasonic extrusion. *Journal of Physics: Conference Series, IOP Publishing* **181** 012027.

[7] B. LANGENECKER (1966) Effects of Ultrasound on Deformation Characteristics of Metals. *IEEE Transactions on Sonics and Ultrasonics* **13** 1-8.

[8] I. GINDIN, G. MALIK, I. NEKLYUDOV, O. ROZUMNYI (1972) Effect of ultrasonic vibrations on the parameters of the hardening curve for copper single crystals. *Soviet Physics Journal* **15** 192-196.

[9] N. TYAPUNINA, V. BLAGOVESHCHENSKII, G. ZINENKOVA, Y. IVASHKIN (1982) Characteristics of plastic deformation under the action of ultrasound. *Soviet Physics Journal* **25** 569-578.

[10] I. LUM, H. HUANG, B.H. CHANG, M. MAYER, D. DU, Y. ZHOU (2009) Effects of superimposed ultrasound on deformation of gold. *Journal of Applied Physics* **105** 024905.

[11] V.G. SUSAN, M.M. DUMITRAS, P.G. ILIESCU (2007) Experimental research of the ultrasonic softening in cold-rolled steel strips. *Surface Engineering and Applied Electrochemistry* **43** 65.

[12] Z. YAO, G.Y. KIM, Z. WANG, L. FAIDLEY, Q. ZOU, D. MEI, Z. CHEN (2012) Acoustic softening and residual hardening in aluminum: modeling and experiments. *International Journal of Plasticity* **39** 75-87.

[13] H. HUANG, A. PEQUEGNAT, B.H. CHANG, M. MAYER, D. DU, Y. ZHOU (2009) Influence of superimposed ultrasound on deformability of Cu. *Journal of Applied Physics* **106** 113514.

[14] A. RUSINKO (2011) Analytical description of ultrasonic hardening and softening. *Ultrasonics* **51** 709-714.

[15] A. RUSINKO, K. RUSINKO (2011) “Plasticity and Creep of Metals”. Springer Science & Business Media.

[16] A. KULEMIN (1978) “Ultrasound and Diffusion in Metals”. Metallurgiya, Moscow.